Optics and Lasers in Engineering 108 (2018) 15–18

Contents lists available at ScienceDirect

Optics and Lasers in Engineering

journal homepage: www.elsevier.com/locate/optlaseng

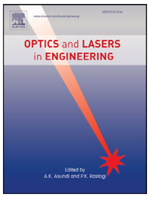

Suppressing the noise in binarized Fourier single-pixel imaging utilizing defocus blur

Ming-Jie Sun[a,b,*], Ji-Yu Huang[a], José Penuelas[b,c]

[a] School of Instrumentation Science and Opto-electronic Engineering, Beihang University, Beijing 100191, China
[b] Laboratoire international associé, Beihang University, Beijing 100191, China
[c] Institut des Nanotechnologies de Lyon, Université de Lyon, UMR 5270, CNRS, Ecole Centrale de Lyon, 36 avenue Guy de Collongue, Ecully Cedex F-69134, France

ARTICLE INFO

Keywords:
Single-pixel imaging
Sinusoidal structured illumination

ABSTRACT

Sinusoidal Fourier patterns are one of the orthogonal basis patterns used in single-pixel imaging. By retrieving the complex Fourier coefficients with phase-shifting algorithm, it reconstructs the image of a scene using inverse Fourier transform. It has been shown that Fourier single-pixel imaging is particularly well-suited to non-conventional imaging applications. However, the frame rate of Fourier single-pixel imaging system is limited because the Fourier patterns are grayscale while the digital micromirror device performs binary modulation much faster than grayscale modulation. The fast Fourier single-pixel imaging addressed the problem by binarizing the patterns, however, the quality of the reconstructed image is jeopardized by the extra induced noise. Here we proposed to suppress the binarization induced noise while keeping the high-speed merit by deliberately applying a precomputed defocus. Numerical simulation and experimental results showed that the proposed method reconstructed images with an averaged 12% lower root mean squared error and ~90% higher signal-to-noise ratio than the fast Fourier method did. To some extent, the proposed method overcame the limitation of the quality-speed trade-off in Fourier single-pixel imaging and made both low noise and high frame rate available simultaneously.

1. Introduction

As a common imaging technique, digital cameras use a detector array to record the light intensity of the image formed by a camera lens. However, before detector arrays were invented, researchers developed imaging techniques using just a single-pixel detector, two of the earliest examples were the flying-spot camera patented by Paul Nipkow and the ‘Televisor’ pioneered by John Logie Baird in 1926, both of which provided a method for encoding and transmitting image information using light modulating masks.

Entering the 21st century, the so-called single-pixel imaging [1–3], closely related to ghost imaging [4–6], raised the interests of the imaging community again due to the advent of micro-electro-mechanical system (MEMS) and micro-opto-electro-mechanical system (MOEMS) devices, which provides a digital means of spatial light modulation. Though not performing as well as digital cameras in the visible spectrum, single-pixel imaging is particularly well-suited to non-conventional imaging, such as multi-wavelength imaging [7,8], depth mapping [9–11], and terahertz imaging [12,13].

One important issue in single-pixel imaging is how to modulate the image, or to structurally illuminate the scene, depending on different set-ups of the system. Earlier ghost imaging schemes used random patterns, generated either from a rotating ground glass [5,14] or a spatial light modulator (SLM) [2,15], for structured illuminations. These schemes require a large number of measurements to reconstruct an image because the randomly generated patterns are partially correlated. Provided the scene is sparse, compressive sensing [16,17], which uses patterns from matrixes satisfying the restricted isometry property (RIP) [18], enables image reconstruction with a much smaller number of measurements at the expanse of a computational overhead.

Recent works [19–22] used patterns from orthogonal basis, which theoretically guarantee perfect reconstructions by fully sampling the scene, and therefore yielded high quality images with less acquisition time. Hadamard basis patterns [23] and Fourier basis patterns [19,24] are two representative choices, the former of which are binary patterns and the latter are grayscale. From a practical point of view, binary Hadamard patterns can be displayed approximately 100 times faster than 8bit grayscale Fourier patterns, if both were displayed on a digital micromirror device (DMD), which is the fastest SLM for the time being. Fast Fourier single-pixel imaging technique [25] was proposed to display Fourier basis patterns, which were binarized using the Floyd-Steinberg error diffusion dithering method [26], on DMD with binary mode. However, extra noise was inevitably induced in the reconstruc-

---

* Corresponding author at: School of Instrumentation Science and Opto-electronic Engineering, Beihang University, Beijing 100191, China.
E-mail addresses: mingjie.sun@buaa.edu.cn, sunmingjiecn@163.com (M.-J. Sun).

https://doi.org/10.1016/j.optlaseng.2018.04.013
Received 29 January 2018; Received in revised form 9 April 2018; Accepted 21 April 2018

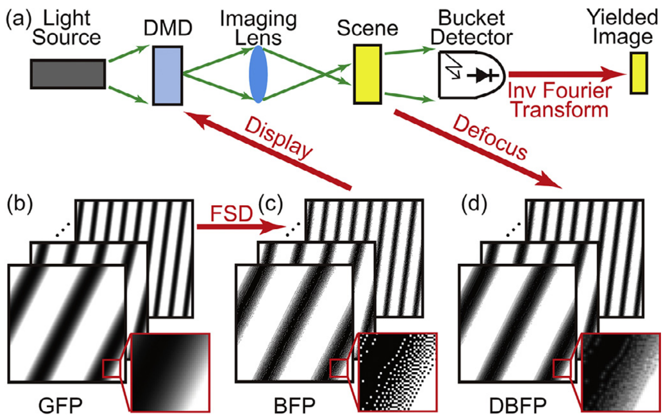

Fig. 1. (a) Defocused Fourier single-pixel imaging scheme. (b) A set of grayscale Fourier patterns (GFP) were generated. (c) The Floyd–Steinberg error diffusion dithering was applied to binarize the GFP to binary Fourier patterns (BFP). The BFP were displayed on the DMD and projected by an imaging lens to provide structured illumination on the scene. (d) The scene was located at a defocus position, therefore the BFP became defocus blurred binary Fourier patterns (DBFP). The bucket detector measured the total light intensities of different patterns and obtained the complex Fourier spectrum of the scene. By performing inverse Fourier transform, an image was reconstructed.

tion images because the binarized Fourier patterns were only approximations to the grayscale ones. As a result, a trade-off exists between the image quality and the imaging speed of the Fourier single-pixel imaging system.

In order to suppress the noise of the reconstructed images while keeping the high-speed merit of using binarized Fourier basis patterns, we deliberately applied a precomputed defocus in the fast Fourier single-pixel imaging system. Numerical simulation and experimental comparison demonstrated that the defocus blurred binary Fourier patterns exhibited a better approximation to the grayscale Fourier patterns than the focused binary ones did. Consequently, by analyzing the results of 35 images reconstructed using the proposed method revealed an average 12% lower root mean squared error (RMSE) and 92% higher signal-to-noise ratio (SNR) than without defocusing.

2. Theory

In Fourier single-pixel imaging (Fig. 1a), the structured illumination is performed with grayscale Fourier patterns (GFP, Fig. 1b), each of which follows a sinusoidal distribution and is characterized by its two-dimension frequencies f_x, f_y, and initial phase ϕ as:

$$P_\phi(x, y; f_x, f_y) = a + b \cdot \cos\left(2\pi f_x x + 2\pi f_y y + \phi\right), \tag{1}$$

where x and y are the two-dimensional coordinates, a and b are the DC term and contrast of the pattern, respectively. The patterns are sequentially displayed on a DMD, and then projected onto the scene as structured illumination. The four-step [19] or three-step [27] phase-shifting algorithm is applied to obtain the complex Fourier coefficients of different frequencies f_x and f_y to retrieve the Fourier spectrum of the scene. An image of the scene can be reconstructed by applying inversed Fourier transform on the spectrum. However, since the GFP are grayscale, they cannot be displayed on the DMD at its maximum rate (~22 kHz, binary mode) but only 290 Hz (8 bit mode). To take full advantage of DMD's high modulation rate, Zhong et al [25] proposed to upsample the GFP (enlarging them without interpolation) then perform binarization using the Floyd–Steinberg error diffusion dithering method [26] to get binary Fourier patterns (BFP, Fig. 1c) which have approximate intensity distributions to the GFP. However, binarization causes quantization errors to the patterns, and the retrieved complex Fourier coefficients are less accurate, which induced extra noise and jeopardized the quality of the reconstructed images.

Though considered to be a negative effect in most imaging applications, defocus can be useful for certain applications, such as depth estimation using defocusing [28,29]. The intensity distribution of a defocused point can be modeled as a two-dimensional Gaussian [30]:

$$G(x, y) = \frac{1}{2\pi\sigma^2} e^{-\frac{x^2+y^2}{2\sigma^2}}, \tag{2}$$

where σ is the standard deviation of the Gaussian distribution. The defocus blurred image can be calculated as the convolution of the Gaussian distribution and the focused image.

Usually, the scene is placed at the focus plane of the DMD, determined by the projection lens. In this work, our hypothesis was that the defocused binary Fourier patterns (DBFP, Fig. 1d) had better approximation to the GFP than the BFP did. The Floyd–Steinberg dithering binarizes GFP into black and white dots and represents grayscale values of GFP by using certain proportions of the black and white dots. When being defocused, the sharp, high-contrast edges between the black and white dots become gradual transitions in grayscale due to the point spread function modeled as a two-dimensional Gaussian. In the Fourier single-imaging system set-up, the scene was moved away from the focus object plane to a precomputed defocusing position (Fig. 1a) and therefore would be structurally illuminated by the DBFP. If our hypothesis stood, more accurate complex Fourier coefficients and higher quality images will be yielded by using DBFP than by using BFP.

3. Results

To reconstruct an image with 128 × 128 pixels in Fourier single-pixel imaging, a complete set of GFP will be generated, each of which has the pixel resolution of 128 × 128. For $\phi = 0$, the total number of the set was 128 × 128 / 2 = 8192. These patterns were upsampled to $k128 \times k128$ pixel resolution by a factor of k using 'bilinear' interpolation before the Floyd–Steinberg error diffusion dithering was performed to binarize them. A larger k leads to a better approximation, however, in practical a larger k also means a higher pixel resolution, and in single-pixel imaging systems the noise of the reconstructed image is more severe as the resolution is increased [20]. Following the conclusion of a previous work [25], we set $k = 2$ in this work and generated Fourier binary patterns of 256 × 256 pixel resolution.

3.1. Numerical simulation

In the numerical simulation, the defocus blur was performed by convoluting the binary patterns with a discrete Gaussian kernel determined from Eq. (2). Different σ represented different degree of defocus in DBFP and led to different approximation to their corresponding GFP. We increased σ from 0.1 to 2.5 with the increment of 0.02, and for each σ we calculated the RMSE between each DBFP and its corresponding GFP to determine which σ yielded the closest approximation for the pattern.

Fig. 2a showed that the numbers of the DBFP reached their minimum RMSEs at different values of σ. 2823, 2386 and 1078 DBFP were defocused into the closest approximation to their corresponding GFP when the values of σ were 0.78, 0.80 and 0.82, respectively. The total patterns for these three values took up 76.8% of the set, therefore we chose $\sigma = 0.8$ as the best defocusing value. Fig. 2b showed that at $\sigma = 0.8$, the DBFP had smaller RMSEs (averaged RMSE 0.086) to the GFP than their corresponding BFP did (averaged RMSE 0.371), which verified our hypothesis that the defocus blur yielded a better approximation to the GFP.

After determining the best σ for defocus, simulation of image reconstruction was performed using all three sets of patterns, i.e. GFP, BFP and DBFP. We used the four-step phase-shifting algorithm [19], where ϕ was set to 0, $\pi/2$, π and $3\pi/2$ respectively, to obtain the complex Fourier spectrums and reconstructed the images by applying inversed Fourier transform on the spectrums. A group of 35 digital photographs were used as 35 different objects in the simulation and Fig. 3a showed